Status of ArgoNeuT, a study of ν-interactions using a Liquid Argon TPC in the NuMI beam at Fermilab.

Carl Bromberg
Michigan State University, East Lansing, MI 48824

E-mail: bromberg@pa.msu.edu

Abstract. The Liquid Argon Time Projection Chamber (LArTPC) technology is a leading candidate for a 100-kiloton class detector for electron neutrino appearance in a long-baseline muon-neutrino beam and for nucleon decay within the stable Argon nucleus, both with excellent efficiency and background rejection. The US has taken its first steps toward development of the technology by constructing and operating small LArTPC detectors, the latest being the ¼-ton detector of the ArgoNeuT collaboration. In a recent 6-month run in the low-energy configuration of the NuMI neutrino beam at Fermilab, the collaboration recorded a large sample of neutrino events. This paper reports on the characteristics of that data, the preliminary steps to reduce the data to a sample of neutrino-induced events, and a description of an event consistent with a charged current quasi-elastic electron-neutrino interaction.

1. Introduction

The Liquid Argon Time Projection Chamber (LArTPC) technology developed within the context of the ambitious ICARUS project [1] has not as yet convincingly demonstrated (at least in the US) that the technology could fulfill its promise to provide excellent efficiency and background rejection for neutrino and proton decay physics at a reasonable cost. Over the last 5-6 years has there been a growing community of physicists and engineers who felt that with a staged approach [2] a convincing case could be made for the construction of a large detector [3] in the U.S. After two groups

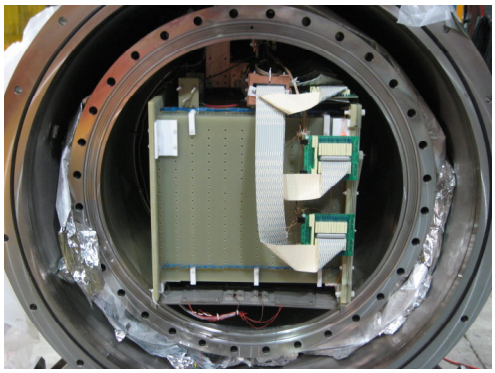

Figure 1. ArgoNeuT detector in its cryostat with the cathode on the left, wire planes on the right. The signal cables terminate on the bias voltage distribution cards.

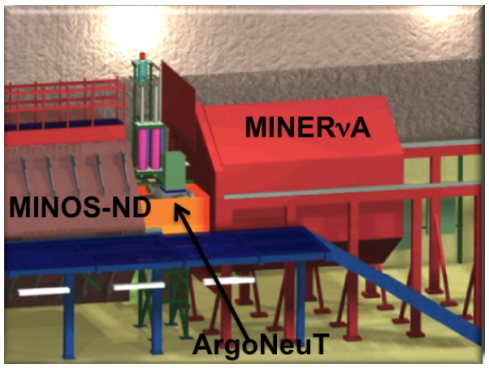

Figure 2. ArgoNeuT LAr-containment box, RF-shielding box, and cryogenic purification system, between the MINOS and MINERVA detectors.

successfully tested small LArTPC prototypes [4] the ArgoNeuT collaboration proposed Fermilab T962 [5], a joint NSF and DOE supported R&D project to build and operate a 170 liter (active volume) LArTPC detector, as shown in figure 1, and conduct a program of neutrino cross-section measurements, utilizing Fermilab's 270 kW neutrino beam. Of particular interest are the cross sections for charged current quasi-elastic (CCQE) neutrino scattering.

After testing on the surface the ArgoNeuT detector was installed in the NuMI Near Hall, 100 m below ground, and by the end of the run it had become sandwiched, as shown in figure 2, between the MINERVA and MINOS detectors. The MINOS detector provides momentum and charge sign measurements for energetic forward muons in ArgoNeuT events. Readout was triggered at the beam spill rate (0.5 Hz), thus recording all neutrino interactions in the active region of the detector.

In April 2009 the cryostat was sealed, pumped down and then filled with liquid Argon. A measurement of the statistical noise on the wires yielded an RMS of 1.4 ADC counts with negligible coherent noise. In pure Argon, 4 mm of track length for a minimum ionizing particle should have a mean signal amplitude of ~ 35 ADC counts in the Collection plane and ~ 17 ADC counts in the Induction plane. Thus a signal to noise of at least 10 to 1 was expected. However, during the Spring

Figure 3. Snowflake comprised of tracks from an ArgoNeuT event display, below.

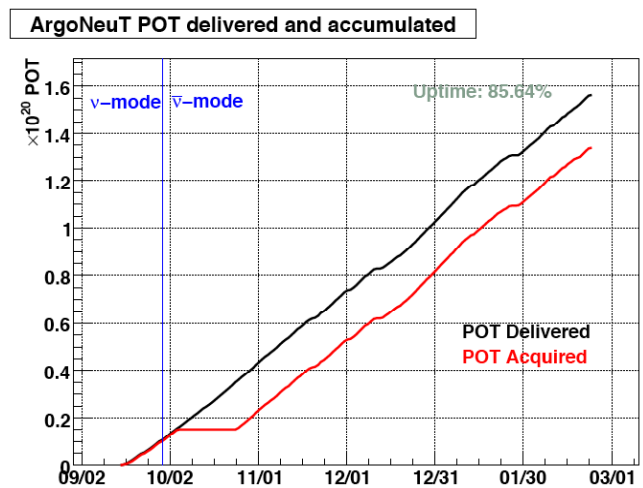

Figure 4. ArgoNeuT beam usage starting in the Fall of 2009. The beam was changed to anti-neutrinos in late Sept, and the majority of the data is in that mode.

2009 running, the electron lifetime was not long enough to approach this level of signal to noise over most of the drift region. Nevertheless, a number of clear neutrino interactions were identified and presented at conferences and meetings [6]. These interaction displays could appear in rather unexpected places, such as on Fermilab's 2009 Season's Greetings card, as shown in figure 3. Though not currently being analyzed, some of this early data may become useful in the future.

During the accelerator shutdown in summer 2009, the electron lifetime was improved, reaching ~ 750 μs as measured in an analysis to be described later but it was not possible to open the cryostat to address the electronics issues to be discussed later. In the subsequent running, except for a 2½-week period in October with a cryogenics problem, the experiment acquired data for 1.5×10^{19} protons on target (POT) in the neutrino mode and 1.2×10^{20} POT in the anti-neutrino mode, as shown in Figure 4. This running should yield in the fiducial volume of the TPC approximately 900 ν Charged Current (CC) interactions in the NuMI neutrino-beam configuration, and 4000 ν and 3500 $\bar{\nu}$ CC interactions in the antineutrino-beam configuration.

2. Electronics and raw data

The analog readout electronics built specifically for the ArgoNeuT detector included a dual jFET front-end integrating preamplifier followed by high- and low-pass filters, implemented on 16-channel

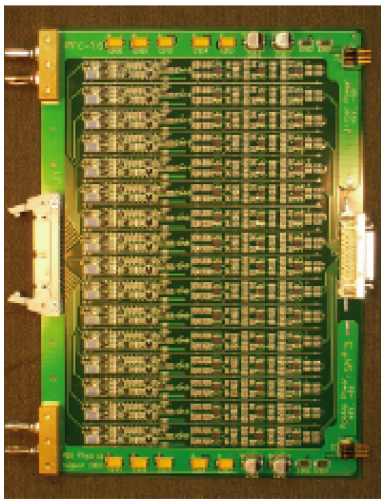

Figure 5. 16-channel preamplifier card with dual jFET front-end, pulse shaping high-pass and low-pass filters, and a cable driver.

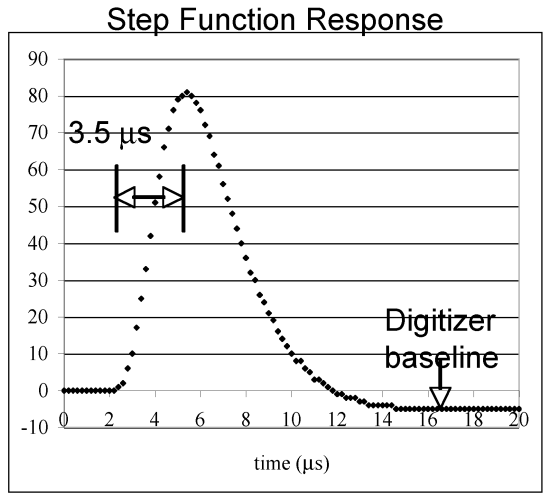

Figure 6. Response of the combined filter and digitizing electronics to a step-function signal at the integrator (a delta function signal on the wire)

cards, as shown in figure 5**.** These were mounted in a double-walled RF-shield cage enclosing the cards and the signal feed-through. Existing ADF2 32-channel digitizers [7] were borrowed from spares of the D0 experiment. With the limited number of available digitizer channels (480), 4 mm was chosen for both pitch and plane separation of the three TPC wire planes, Shield, Induction, and Collection, with the wire angles, 0°(vertical), and ±30°, respectively. Only the latter two planes were instrumented, each with 240 channels of readout. The signal on each wire was digitized at a 5 MHz rate for a total of 406 µs beginning 10 µs before the start of a 10 µs long NuMI beam spill. It takes ~310 µs to drift the 470 mm distance between the Cathode and Grid wire planes, in the 500 V/cm electric field established between them.

After pulse shaping, the signal for an ionizing track has a rise time of at least a few microseconds, but the capacitive coupling of the digitizer inputs, which could not be modified, were designed for signals ~100 times shorter. In addition, a series resistor compensating for gain differences between ADF2 channels modulated the effects of this capacitive coupling. For the combined shaping circuit and digitizer input, the step-function response, as shown in figure 6, had a peaking time of ~ 3.5 µs with a negative baseline shift of 7-10% of the signal amplitude with a decay constant of 50–100 µs.

There were a number of unique features of the electronics implementation for this LArTPC. Bias voltages were distributed via 1 MΩ resistors to each wire (Shield at -298 V, Induction at -18 V, Collection at +338 V) and decoupled with capacitors feeding the low-voltage signal cables via TPC mounted cards (see figure 1), submerged in the liquid Argon. Through testing in Fermilab's Materials Testing Station [8] we know that these components will not contaminate liquid Argon.

Without the need to carry a bias voltage, the cables and a new feedthrough could use mass-terminated connectors. We were disappointed to later find that the feedthrough had a number of flaws that caused ~5 dead or noisy channels, which could not be repaired. Also, there were no signals from 5 sequential wires in the Collection plane resulting in event displays that exhibit a noticeable gap in tracks crossing this region. The wires neighboring this region collect more charge than expected, indicating that these dead Collection plane wires did not receive bias voltage. No signal shape distortions were seen for the corresponding ionization in the Induction plane. Finally, the bias voltage

cards had small un-insulated spots on traces where charge could be collected from outside the active TPC volume. This could generate, primarily on the last 48 wires of the Induction plane (right hand corner in displays), a strange signal with the wrong polarity. Though distracting, these signals are rare in events of interest, and are not present in the other view and thus do not reconstruct in 3D.

After the summer shutdown, coherent noise became more noticeable and reached a peak of about 1.0 ADC counts. As the data to be presented below will clearly indicate, none of the problem areas described here are serious enough to prevent ArgoNeuT from achieving its physics goals

3. Constructing hits

On each wire, track signals are separated from noise by application of a hit threshold. In the raw data, the negative portion of a bipolar signal in the Induction plane or the negative baseline shift of a signal in the Collection plane can cause the positive portion of a subsequent signal to drop below a hit threshold. To insure that a hit threshold is uniformly efficient, a Fast Fourier Transform (FFT) deconvolution was employed to minimize these effects. The deconvolution removes the baseline shift from the Collection plane signals and converts the raw signals in the Induction plane from bipolar to unipolar. Also, some improvement in the signal to noise ratio in the Induction plane can be obtained with this procedure.

This FFT deconvolution technique makes the assumption that every true signal on a particular wire can be resolved into components that to first order have the same base signal shape in time. Ionization electrons follow different paths as they drift through the wire planes, contributing different shapes to the overall signal. The quality of the deconvolution, therefore, depends on the details of the signal formation, which are different in the two readout planes. The majority of the signal on a Collection plane wire is due to ionization from a projected track length equal to the wire pitch, centered on the wire, and generated rather close to the wire. Therefore, the invariance of the component shapes contributing to Collection plane signals is a particularly good approximation.

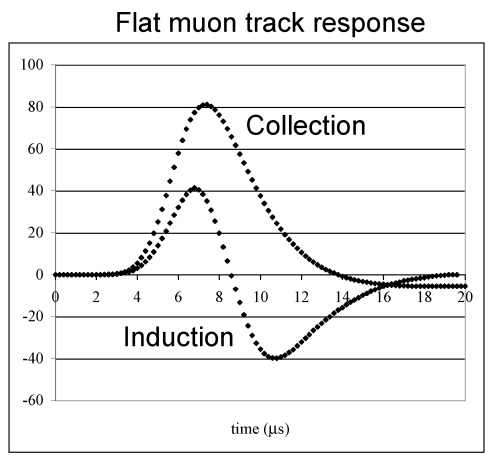

Figure 7. Base signal shapes for the Collection and Induction planes as determined from muon tracks parallel to the wire planes.

Signals on Induction plane wires, however, contain significant components from ionization that will be closer to a neighboring wire when passing through the plane. That distant charge will make contributions to the signal with a shape different from that of charge passing closer to the wire. These shape differences (the utility of which is minimized by ionization fluctuations) are washed out by the frequency response of the electronic shaping circuits that favor better signal to noise. The variations in the shape of the digitized Induction plane bipolar signals are not large. For example, the ratio of the positive to negative amplitude of the bipolar signal generated by isolated tracks rarely varies by more than ±15% from the base signal shape. These variations can generate deconvolution artifacts, however, they are small enough that a common signal shape is an adequate first approximation for hit finding. A better approximation to the signal shape is possible, once the angles, ionization, and density of the tracks are known.

The base signal shapes for the Collection plane and Induction plane wires, as shown in figure 7, were derived from thousands of spills containing a long muon track nearly parallel to the wire planes. Track segments with signals with a wider pulse than expected, indicating the presence of a delta ray, were not included in the signal shape determination. As a side benefit of using muon tracks for the signal shape on each wire, the deconvolution can be adjusted to result in signal amplitudes on each

wire normalized to a common ionization scale. These muon track signals should have the shortest rise time of any ionization deposition by a track.

Another aspect of the FFT technique used here is the frequency filter. The filter used in the Collection plane was based on the power spectrum of the base signal. Due to the slowly varying baseline shift, this filter must accept low frequencies. In the Induction plane, baseline variations are quite small so that a filter with a low frequency cut-off could be used.

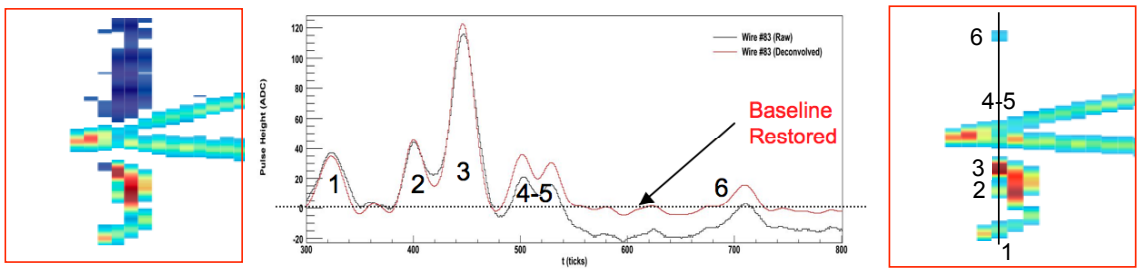

Figure 8. Collection plane signals are shown in the vertex region of a two-prong neutrino interaction. The raw data display (left panel) exhibits pulse heights far below the baseline (dark blue). Signals on wire 83 (center panel) before and after (black/red) the deconvolution, and the display (right panel) following deconvolution, wire 83 indicated by the vertical line.

A few examples will illustrate the capabilities of the signal deconvolution procedure. To demonstrate the effects of the signal deconvolution in the Collection plane, the vertex region of a 2-prong neutrino interaction is analyzed in detail, as shown in figure 8. The signal peak #3, likely due to a photon conversion, has ionization ~ 4 times the minimum and the raw data has depressed the baseline, lowering the pulse heights of hits 4-5 and 6. The deconvolution has restored the baseline, raising the pulse heights of peaks 4-5 to a level consistent with minimum ionizing tracks, and hit 6 is

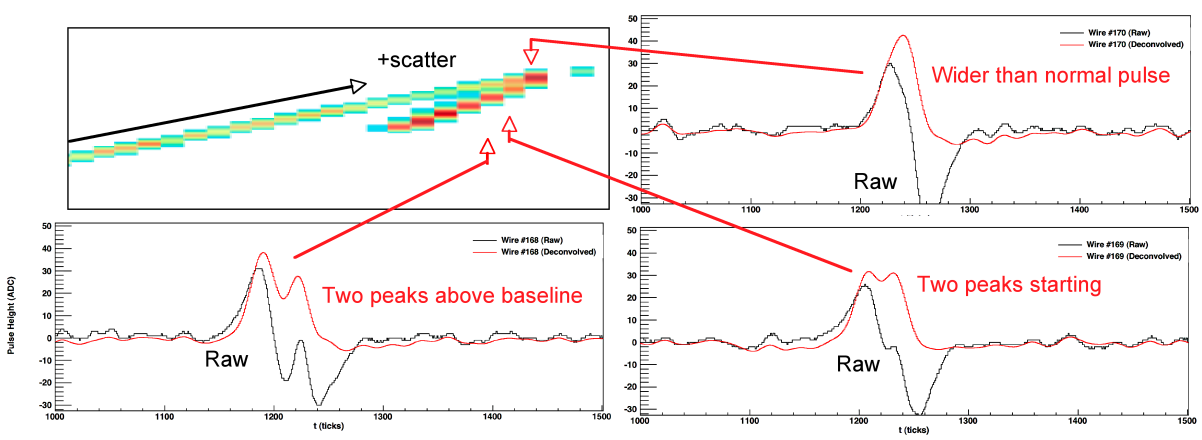

Figure 9. Deconvoluted Induction plane view of a scattered track (upper-left). Also shown are the wire views on three consecutive wires (168–170) with the raw data in black and deconvoluted signals in red. Note: Induction plane pulse heights are typically ½ those of the Collection plane.

now above the hit threshold. In the same event the upper track scatters backward and stops in the active volume, as shown in the upper-left panel of figure 9. Also shown are wire displays for three consecutive Induction plane wires, illustrating that the deconvolution procedure has extracted the signal of the incoming track from the negative portion of the raw bipolar signal of the scattered track.

4. Cluster and track finding

The hit finding described above and the description of the 2D and 3D reconstruction that follows have their software codes packaged in LArSoft [9], a Fermilab supported framework for the LArTPC activities in the US. Once hits are found in the 2D projections, they are grouped in each view into "clusters" using a DBSCAN [10] algorithm. A Hough Transform [11] algorithm applied to the hits within a cluster find those hits that lay along straight-line tracks. The minimum number of missing hits and allowed deviation of a hit from the track are adjustable parameters, initially set at values optimized for efficiency. Both wire planes cover the active volume of the TPC completely, thus a track identified in the one view that enters or leaves the TPC active volume will have a corresponding endpoint with a common drift coordinate in the other view. This provides nearly unambiguous matching of the tracks in the two views. Through-going tracks entering on one boundary and leaving through another have two such corresponding endpoints in 3D.

A neutrino interactions in the material outside the active TPC volume generate all species of particle, however, nearly all of those that enter and then leave the active region of the TPC are muons.

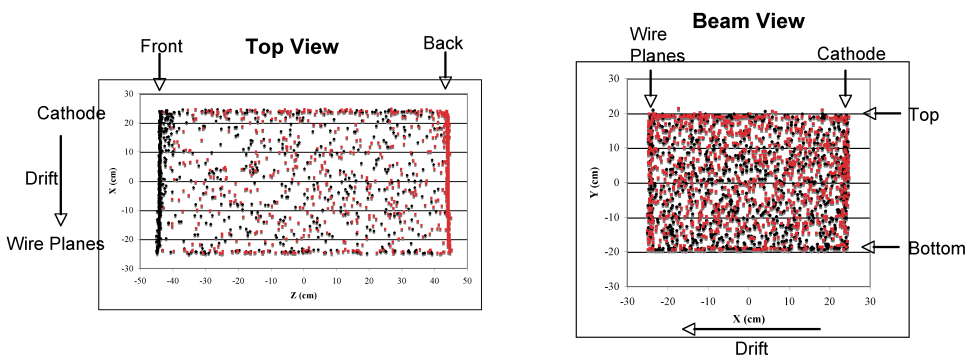

Figure 10. Reconstructed endpoints for muon tracks that enter and leave the TPC active volume, upstream points plotted in black, and downstream points in red. Field distortions (see text) are responsible for the inward tilt for the front and back.

As a first quality check on the reconstruction, about 60,000 beam spills were used to identify a large sample of straight tracks where both endpoints could be reconstructed in 3D. The endpoints should mark the boundaries of the active volume, as shown in figure 10. In the frame labelled Top View, many tracks enter the front (upstream) face or leave the back (downstream) face, at Z = ±45 cm of the TPC. Also, the endpoints show that there are tracks that leave or enter through the Cathode or wire planes at X = ±23.5 cm. Unexpectedly, the boundaries of the front and back surfaces of the TPC look further apart near the wire planes than they do near the Cathode (longest drifts). However, a map of the electric field reveals that some field lines at the edges of the cathode do not end on the wire planes.

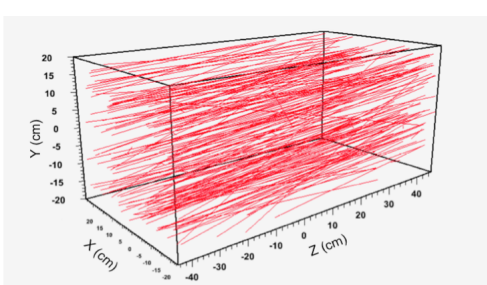

Figure 11. Muon tracks reconstructed in 3D by matching all 2D hits between views, and superimposing tracks from many spills.

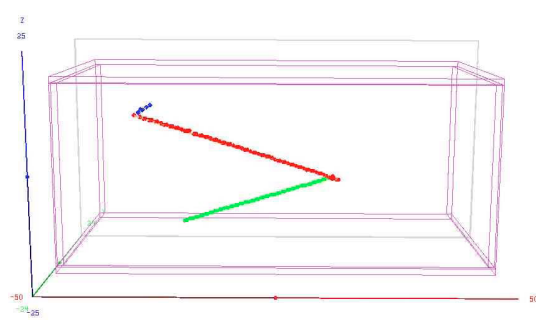

Figure 12. The 2-prong neutrino event shown earlier is displayed with the tracks reconstructed in 3D.

A region about 1 cm inboard from the field-cage is therefore inactive, except close to the wire planes where field lines from the two nearest field-cage electrodes can carry charge to the wires.

The points that lie well within the boundaries of the TPC in the Top View must enter or leave though its top or bottom. This is confirmed in the plot labelled Beam View, where there are concentrations of endpoints on the top and bottom of the TPC. A few reconstructed endpoints appear to lie just outside the top surface of the TPC at Y = + 19.5 cm. The y-coordinate is the least well known of the three coordinates. For endpoints off by 1-2 wires in the two views the y-coordinate can reconstruct up to 16 mm from the true endpoint, consistent with the deviations of those few tracks from the nominal top boundary.

Another approach to 3D reconstruction matches all hits between the two views based on a common drift time. The algorithm works particularly well on isolated tracks such as muons, as shown in Figure 11. Low multiplicity neutrino interactions, such as the two-prong event described earlier in Section 3, are reconstructed with the same algorithm in 3D, as shown in figure 12. Work continues to develop code that will reconstruct tracks in nearly all events in 3D.

5. Electron lifetime from muon tracks.

Using the straight track reconstruction algorithms described above, a selection of minimum ionizing muon tracks at least 40 cm long from ~70,000 beam spills (~ 2 days of running) enabled a measurement of the electron lifetime in the liquid Argon. The deconvolution algorithm yielded an

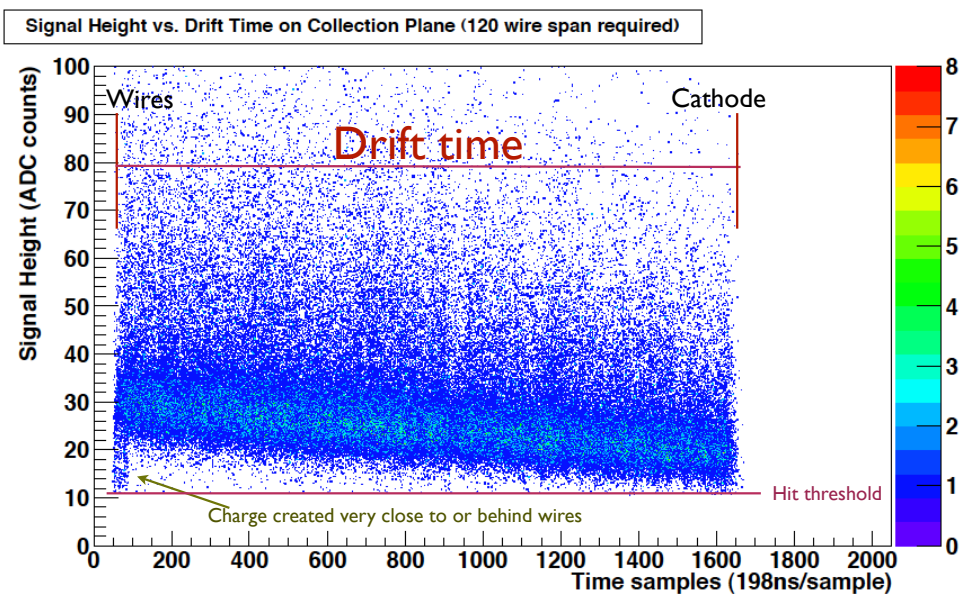

Figure 13. From a single run, the pulse height spectra vs. drift time for tracks reconstructed in the Collection view with at least 120 hits. Electron lifetime effects on the most probable pulse height are clearly demonstrated.

ionization measurement of every hit, normalized in ADC counts to an average of the signal pulse heights in each plane. A plot of the ionization of each hit vs. its drift time, as shown in figure 13, at a fixed drift time exhibits the expected Landau (like) distribution, albeit with smearing induced by instrumental effects and muon track variations in momentum and angle, however, these effects do not vary significantly over the full drift time.

The pulse height spectra in 1.6 μs time slices were selected and excellent fits to a Landau plus a Gaussian-smearing distribution were obtained. From these fits in the Collection plane, excluding drift times near the wire planes or the Cathode, the most probable pulse height plotted vs. drift time, as

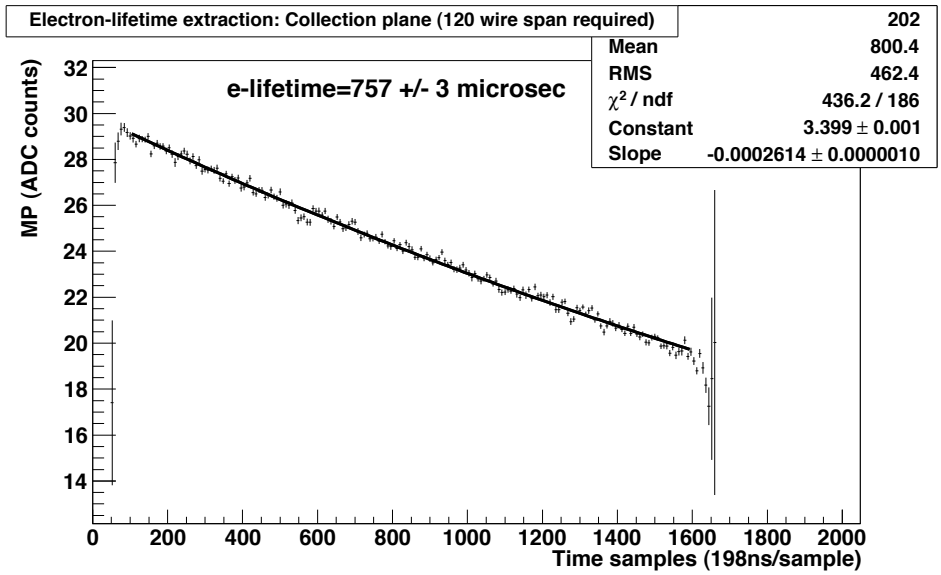

Figure 14. The plotted points are from fits to the most probable pulse height in 1.6 μs slices from the previous figure. The exponential fit for the electron lifetime was restricted to the central time samples where the pulse heights are unaffected by the hit threshold or other instrumental effects. The Slope parameter is the inverse of the lifetime (in time-samples).

shown in Figure 14, exhibits the expected exponential fall with a fitted lifetime of 757 ± 3 μs (statistical error). In the Induction plane a fit yields a similar value when hits affected by a threshold cut are eliminated. The rather poor fit chi-squared, 436 for 186 degrees of freedom, suggests that the fitted mean pulse heights have additional variations not included in the error from the fit in the most probable pulse height from each time slice. One possible source is coherent noise correlated with the common start for the beam spill and the drift time clock.

6. Identification of neutrino interactions

With the muon track 3D reconstruction as described above, a filter removed spills that did not show data consistent with a neutrino interaction. Spills were eliminated if they showed no tracks or just a single straight muon track that enters and leaves the fiducial volume. After removing the ionization of any single muon track, spills were retained for later scanning with more than the ionization equivalent of a 40 MeV energy deposition. During nominal neutrino beam conditions, the filter selects ~3% of the original beam spills. Applying additional cuts in a visual scan, about 25% of these spill records, or less than 0.7% of the original sample, were identified as having a candidate neutrino interaction, and about half of these have unmistakable neutrino interactions with more than 1 charged track at an interaction vertex. The additional cuts applied in the visual scan address cases where there are multiple tracks, most which intersect the front or sidewalls of the TPC, and likely originate outside the TPC. Many of the criteria applied in the visual scan can be coded to reduce the scanning load while others would require more sophisticated reconstruction algorithms to maintain the efficiency in the neutrino event selection. These will be implemented in the near future.

The discovery of CP violation in electron neutrino appearance experiments will require the excellent pattern recognition and particle identification capabilities of the LArTPC technology. With the ArgoNeuT data we hope to make the first measurement of the electron neutrino content of the NuMI beam in the neutrino and anti-neutrino modes. Over the course of the run, random visual scans identified 1 or 2 events that could be electron neutrino interactions, but they were not definitive. In the visual scan of about 450 of spill records selected by the filter from ~15,000 beam spills (about 12 hours of neutrino beam running) an event was found that displayed all the expected characteristics of a charged-current quasi-elastic interaction of an electron neutrino.

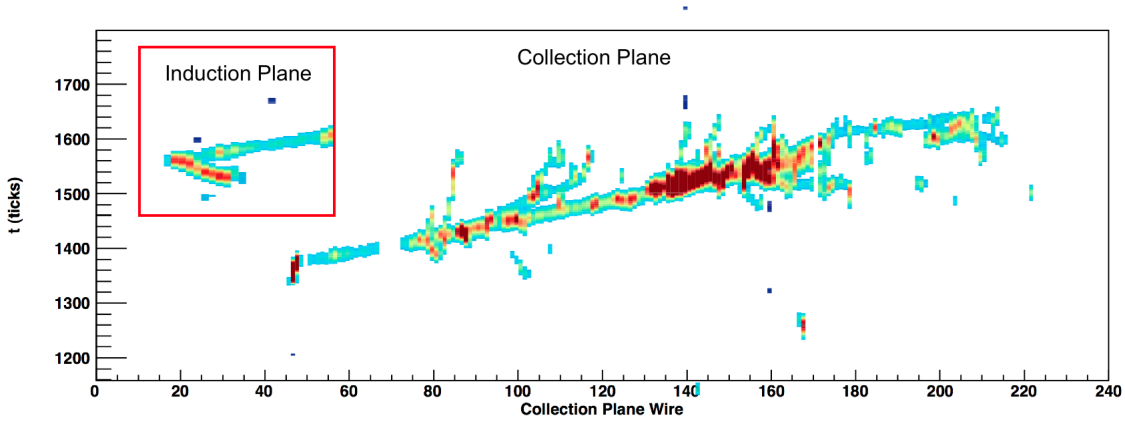

Figure 15. A candidate for an electron neutrino CCQE event shown in the ArgoNeuT Collection plane with one short and heavily ionizing track, and a minimum ionizing track about ~ 11 cm long (big gap is due to 5 dead wires) that develops into an electromagnetic shower. In the Induction plane (inset), the short (~ 5 cm) stopping track and an uninterrupted minimum ionizing track are clear.

The event in the Collection plane, as shown in figure 15, has a two-prong vertex with one minimum ionizing track about 11 cm long (gap is due to 5 consecutive dead wires) that develops into a collinear electromagnetic shower, thus is likely an electron, and a short highly ionizing track that stops in the Argon. The stopping track, more easily seen in the Induction plane (inset), is about 5 cm long and is likely a proton with a kinetic energy of about 85 MeV. Also, the event exhibits no other electromagnetic activity that could be associated with an additional photon of significant energy, e.g., from π^0 or η decays. We continue to scan for additional electron neutrino events. Analysis of the ionization will provide a measurement of the electromagnetic shower energy deposited in the active volume and verification that the stopping track is a proton.

7. Conclusion

The ArgoNeuT collaboration has constructed a 175-liter Liquid Argon TPC, readout by 60°-stereo wire planes, each with 240 wires on a 4-mm pitch. The electronics exhibited an average statistical noise of 1.4 ADC counts with minimum ionizing tracks producing at the midpoint of the drift distance a mean signal amplitude per 4 mm of track length of 31.5 ADC counts in the Collection plane, and 15.5 ADC counts in the Induction plane.

The experiment recently completed a 6-month run at Fermilab in the NuMI beamline in a low-energy configuration providing neutrinos with a mean energy of 3.5 GeV. This run should yield within the fiducial volume ~ 900 ν Charged Current (CC) events in the neutrino beam mode, and ~ 4000 ν and ~ 3500 $\bar{\nu}$ CC events in the antineutrino beam mode. Work is in progress to obtain the momentum and sign of most muons by linking tracks in the LArTPC with the MINOS near detector. The energy determination for electromagnetic showers will be investigated through reconstruction of π^0 decays. Events have been seen with the characteristics of ν_e scattering indicating that measurement of the ν_e fraction in the NuMI beam at the ~ 1% level should be possible.

Acknowledgements
The author thanks the GLA2010 conference organizers for the invitation to talk at the conference, and my ArgoNeuT colleagues for help in preparing the data presented here.

References

[1] Cennini P, et al. 1994 *Nucl. Instr. & Meth.* A **345** 230; Arneodo F, et al. 2003 *Nucl. Instr. & Meth.* A **498** 292-311; Amerio S, et al. 2004 *Nucl. Instr. & Meth.* A **527** 329.

[2] Fleming B T 2009 Liquid Argon TPC for LBNE, DUSEL workshop, Homestake, SD, BFleming-DUSELWorkshopFall2009.pdf

[3] Rameika G 2009 Liquid Argon and the Long Baseline Neutrino Experiment (LBNE), Fermilab Director's Review, Rameika_LBNEoverview_LArDirRevNov2009Final.pdf; Baller B 2010 LBNE Liquid Argon option, *in these Proceedings*.

[4] Curioni A, et al. 2008 The Yale liquid argon time projection chamber, *arXiv*:0804.0415; Bromberg C 2009 Review of LAr Electronics R&D at Fermilab, http://lartpc-docdb.fnal.gov/cgi-bin/ShowDocument?docid=412 .

[5] ArgoNeuT: http://t962.fnal.gov/

[6] See for example, Soderberg M 2009 ArgoNeuT:A Liquid Argon Time Projection Chamber Test in the NuMI Beamline, *Proceedings of the DPF-2009 Conference*, Detroit, MI

[7] Bromberg C and Edmunds D 2006 A Modular Readout System for A Small Liquid Argon TPC http://lartpc-docdb.fnal.gov/cgi-bin/ShowDocument?docid=594.

[8] Finley D, et al. 2006 Work at FNAL to acheive long electron drift time in Argon, *FERMILAB-TM-2385-E*; Rebel B 2010 Results from the materials test stand and status of LAPD, *in these Proceedings*.

[9] Rebel B 2009 Introduction to LArSoft,vmsstreamer1.fnal.gov/VMS_Site_03/Lectures/ MicroBoone/presentations/091015Rebel.pdf

[10] Ester M, et al. 1996 A Density-Based Algorithm for Discovering Clusters in Large Spatial Databases with Noise", *The Second International Conference on Knowledge Discovery and Data Mining (KDD-96)*, Portland, Oregon, USA.

[11] Hough P V C 1959 Machine Analysis of Bubble Chamber Pictures, *Proc. Int. Conf. on High Energy Accelerators and Instrumentation*.